

Vibrational Study of Some Layered Structures Based on Titanium and Zirconium Phosphates

Pier Luigi Stanghellini,^{*†} Enrico Boccaleri,[†] Eliano Diana,[‡] Giulio Alberti,[§] and Riccardo Vivani[§]

Dipartimento di Scienze e Tecnologie Avanzate e INSTM, Università del Piemonte Orientale "A. Avogadro", Piazza Giorgio Ambrosoli 5, 15100 Alessandria, Italy, Dipartimento di Chimica IFM, Università di Torino, via P. Giuria 7, 10125 Torino, Italy, and Dipartimento di Chimica, Università di Perugia, via Elce di Sotto 6, 06123 Perugia, Italy

Received April 2, 2004

A Raman and infrared study was carried out on layered zirconium and titanium acid phosphates of α - and γ -type, α -M[O₃POH]₂·H₂O and γ -M[PO₄][O₂P(OH)₂]·2H₂O, respectively. The spectra were initially approached by means of the classical correlation method in the solid state, which accounts for the complexity of the infrared spectra of both species. However, the number of bands and their relative intensity in the Raman spectra suggest a quite total absence of quadrupolar coupling between the vibrating units. So, if interunit coupling is neglected, a molecular approach considering the vibrations of isolated tetrahedral [PO₄] and octahedral [MO₆] building blocks can allow an affordable spectroscopic description of the title compounds. Interesting insights on the relationships between spectral properties and structure can be drawn by comparison with the spectra of alkali phosphates and of MO₆ oxoanions. A significant high-energy shift of the ν (P–O) modes is observed in the layered phosphates with respect to the corresponding salts, which parallels the low-energy shift of the ν (M–O) modes. Surprisingly, an increase of the M–OP interaction can reinforce the P–O bond. A simple theoretical model, based on the interaction between the [PO₄] unit and four Li⁺ in similar geometrical arrangement found in the structures of the layered phosphates, offers a reasonable explanation of this phenomenon.

Introduction

The chemistry of transition metal phosphates and phosphonates has been till now a subject of increasing interest because a variety of compounds with different structures and properties can be prepared.¹ Even by limiting our attention to phosphates and phosphonates of tetravalent transition metals and, among them, only layered structures, the number of already known compounds is very high.^{1,2} All the structures of the above compounds can be easily described

by the combination of octahedral–tetrahedral building blocks in which the transition metal ion, in its octahedral configuration, shares one or more oxygen atoms of tetracoordinated oxoanions of phosphorus.

It is now well-known, for example, that the α -layered structure of metal(IV) bis(monohydrogen phosphates) is generated by MO₆ octahedra, each one sharing its six oxygen atoms with six different monohydrogen phosphate groups. In turn, each HPO₄ group behaves as a tridentate anionic ligand and shares three oxygen atoms with three different metal atoms.³ For this reason the above compounds are often formulated as M(IV)(O₃POH)₂.

Another important structure of M(IV) phosphates is the so-called γ -type layered structure in which equimolar amounts of phosphate and dihydrogen phosphate groups are present. Each phosphate unit behaves as a tetradentate ligand and bridges four different zirconium atoms placed in two different planes belonging to the same lamella. The octahedral coordination of the central metal ion is achieved by

* To whom correspondence should be addressed. E-mail: pierluigi.stanghellini@mfn.unipmn.it. Fax: 0131.287416.

[†] Università del Piemonte Orientale "A. Avogadro".

[‡] Università di Torino.

[§] Università di Perugia.

(1) (a) Clearfield, A. In *Progress in Inorganic Chemistry*; Karlin, K. D., Ed.; John Wiley & Sons: New York, 1998; Vol. 47, p 374. (b) Alberti, G. In *Comprehensive Supramolecular Chemistry*; Alberti, G., Bein, T., Eds.; Pergamon–Elsevier Science Ltd.: Oxford, U.K., 1996; Vol. 7, p 151. (c) Clearfield, A.; Costantino, U. In *Comprehensive Supramolecular Chemistry*; Alberti, G., Bein, T., Eds.; Pergamon–Elsevier Science Ltd.: Oxford, U.K., 1996; Vol. 7, p 107.

(2) (a) Poojary, D. M.; Zhang, B.; Clearfield, A. *Angew. Chem., Int. Ed. Engl.* **1994**, *33*, 2324. (b) Sung, H. H.-Y.; Yu, J.; Williams, I. D. *J. Solid State Chem.* **1998**, *140*, 46.

(3) Clearfield, A.; Troup, J. M. *Inorg. Chem.* **1977**, *16*, 3311.

dihydrogen phosphate groups, which act as bidentate ligands, and are placed on the external parts of the lamellae.⁴ The compounds of this family are therefore formulated as $M(\text{IV})[\text{PO}_4][\text{O}_2\text{P}(\text{OH})_2]$.

From these two typical classes of layered $M(\text{IV})$ phosphates, two large families of organic derivatives, exhibiting similar α - and γ -layered structures, can be obtained by a partial or complete substitution of O_3POH and $\text{O}_2\text{P}(\text{OH})_2$ building blocks with phosphonato (diphosphonato) or phosphinato (diphosphinato) groups such as O_3PR , $\text{O}_3\text{P}-\text{R}-\text{PO}_3$, $\text{O}_2\text{P}(\text{OH})\text{R}$, $\text{O}_2(\text{OH})\text{P}-\text{R}-\text{P}(\text{OH})\text{O}_2$, O_2PR_2 , etc. A great variety of materials with tailor-made properties (solids with a purpose) can be thus prepared just by an appropriate choice of the organic radical R.^{1,2,5} Some of these were of interest for specific applications in different fields such as ion exchange, molecular intercalation, molecular sieving, shape-selective catalysis, proton conduction, nonlinear optics, and preparation of polymer nanocomposites. The literature is very wide and the interested reader is referred to recent reviews.^{1,2,6}

Most of these compounds are very insoluble. Accordingly, X-ray determination of their structure is not an easy task because single crystals of suitable size are rarely obtained. Thus, powder diffraction analysis combined with other spectroscopic techniques [e.g., infrared, Raman, and ³¹P magic-angle spinning (MAS) NMR] have been used to obtain some detailed structural information.⁷ In this connection, laser Raman spectroscopy is a very promising technique to obtain important information on P–O and M–O bonds within the building blocks, on the interactions between themselves, and on the correlations between the vibrational and the structural data. Moreover, the Raman spectrum can be obtained directly on the sample without any chemical manipulation, which can modify the structural arrangement. It seemed therefore of interest to perform a systematic Raman investigation on the various Zr and Ti phosphate and phosphonate compounds.

The present paper reports the data concerning the basic α -Zr(Ti)P and γ -Zr(Ti)P layered systems.

Experimental Section

α - and γ -zirconium and titanium phosphates were prepared as previously reported.^{1,8}

The Raman spectra were recorded on the powdered samples by a Bruker RFS 100 FT-Raman spectrophotometer equipped with a

Table 1. Vibrational Modes of the Building Blocks

	[MO ₆] <i>O_h</i>	[PO ₄] <i>T_d</i>	[O ₃ POH] <i>C_s</i>	[PO ₂ (OH) ₂] <i>C_{2v}</i>
$\nu(\text{O-H})$			A'	A ₁ + B ₁
$\nu(\text{P-OH})$			A'	A ₁ + B ₁
$\nu(\text{P[M]-O})$	A _{1g} + E _g + T _{1u}	A ₁ + T ₂	2A' + A''	A ₁ + B ₂
$\delta(\text{P-O-H})$			A' + A''	A ₁ + B ₁
$\delta(\text{O-P[M]-O})$	T _{1u} + T _{2g} + T _{2u} + T _{1g}	E + T ₂	2A' + A''	A ₁
$\delta(\text{O-P-OH})$			A'	A ₂ + B ₁ + B ₂
$\delta(\text{HO-P-OH})$				A ₁
$\rho(\text{P-O-H})$			A''	A ₂ + B ₂

350 mW Nd³⁺:YAG laser emitting at 1064 nm. Samples were placed in the standard sample holder provided with the instrument. Routine measurements were recorded with 100 scans at 90 mW laser power, at a resolution of 4 cm⁻¹. Measures on Ti-containing samples were recorded at the same resolution with 200 scans at 200 mW laser power.

KBr pellet infrared spectra of salt phosphate moieties were collected by an ATI Mattson Research Series FT IR spectrophotometer. Infrared spectra of the layered systems, avoiding their incorporation in a salt matrix (see below), were recorded by use of a PAS (photoacoustic spectroscopy) accessory on a Perkin-Elmer System 2000 IR spectrophotometer, setting a spectral resolution of 4 cm⁻¹ and acquiring 64 scans. The best results that are reported in this work were obtained on a Perkin-Elmer System 2000 FT-IR equipped with the microscope accessory. The spectra were collected with the microscope in the reflection arrangement, with the standard magnification (20×). The samples were laid on aluminum foil and focused under visible light, and then the spectra were acquired. The spectral resolution was set to 4 cm⁻¹ and spectra were collected over 64 scans.

The ab initio calculation was performed with the Gaussian98 software package. We calculated the energy and harmonic frequencies by using the unrestricted Hartree–Fock method with the 6-31++G(d,p) basis set. The reported calculated frequencies are not scaled.⁹

Results

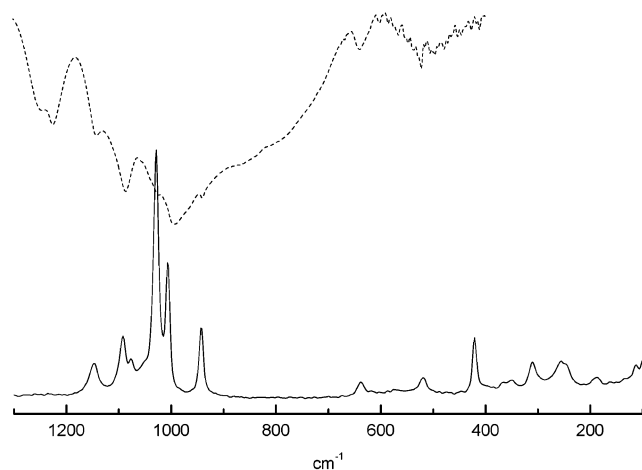
Table 1 summarizes the vibrational modes of the isolated building blocks with their idealized symmetry. These data are the useful basis for a vibrational analysis of the crystal, for which the correlation method¹⁰ is probably the easiest way. Let us use the γ -Zr structure as working example. The relevant data obtained by the structural analysis¹¹ are formula, $\text{Zr}(\text{PO}_4)(\text{H}_2\text{PO}_4)(\text{H}_2\text{O})_2$; crystal system, monoclinic; space group, $P2_1$ (C_2^2); site symmetry, $C_1(2)$; and $Z = 2$. The

- (4) Christensen, A.; Andersen, E. K.; Andersen, I. G. K.; Alberti, G.; Nielsen, N.; Lehmann, M. S. *Acta Chem. Scand.* **1990**, *44*, 865. (b) Poojary, D. M.; Zhang, B.; Dong, Y.; Peng, G.; Clearfield, A. *J. Phys. Chem.* **1994**, *98*, 13616.
- (5) (a) Clearfield, A. In *Design of New Materials*; Cocke, D. L., Clearfield, A., Eds.; Plenum Press: New York, 1987; p 121. (b) Alberti, G.; Casciola, M.; Costantino, U.; Vivani, R. *Adv. Mater.* **1996**, *8*, 291. (c) Alberti, G.; Murcia-Mascarós, S.; Vivani, R. *J. Am. Chem. Soc.* **1998**, *120*, 9291. (d) Alberti, G.; Costantino, U.; Vivani, R.; Zappelli, P. *Angew. Chem., Int. Ed. Engl.* **1993**, *32*, 1357.
- (6) Mallouk, T. E.; Gavin, J. A. *Acc. Chem. Res.* **1998**, *31*, 209.
- (7) (a) Poojary, D. M.; Clearfield, A. *Acc. Chem. Res.* **1997**, *30*, 414. (b) Clayden, N. J. *J. Chem. Soc., Dalton Trans.* **1987**, 1877. (c) Nakayama, H.; Eguchi, T.; Nakamura, N.; Yamaguchi, S.; Danjyo, M.; Tshako, M. *J. Mater. Chem.* **1997**, *7*, 1063. (d) Slade, R. C. T.; Knowles, J. A.; Jones, D. J.; Rozière, J. *Solid State Ionics* **1997**, *96*, 9.
- (8) Alberti, G.; Bernasconi, M. G.; Casciola, M. *React. Polym.* **1989**, *11*, 245.

- (9) Frisch, M. J.; Trucks, G. W.; Schlegel, H. B.; Scuseria, G. E.; Robb, M. A.; Cheeseman, J. R.; Zakrzewski, V. G.; Montgomery, J. A., Jr.; Stratmann, R. E.; Burant, J. C.; Dapprich, S.; Millam, J. M.; Daniels, A. D.; Kudin, K. N.; Strain, M. C.; Farkas, O.; Tomasi, J.; Barone, V.; Cossi, M.; Cammi, R.; Mennucci, B.; Pomelli, C.; Adamo, C.; Clifford, S.; Ochterski, J.; Petersson, G. A.; Ayala, P. Y.; Cui, Q.; Morokuma, K.; Malick, D. K.; Rabuck, A. D.; Raghavachari, K.; Foresman, J. B.; Cioslowski, J.; Ortiz, J. V.; Baboul, A. G.; Stefanov, B. B.; Liu, G.; Liashenko, A.; Piskorz, P.; Komaromi, I.; Gomperts, R.; Martin, R. L.; Fox, D. J.; Keith, T.; Al-Laham, M. A.; Peng, C. Y.; Nanayakkara, A.; Challacombe, M.; Gill, P. M. W.; Johnson, B.; Chen, W.; Wong, M. W.; Andres, J. L.; Gonzalez, C.; Head-Gordon, M.; Replogle, E. S.; Pople, J. A. *Gaussian 98, Revision A.9*; Gaussian, Inc.: Pittsburgh, PA, 1998.
- (10) Fateley, W. G.; Dollish, F. R.; McDevitt, N. T.; Bentley, F. F. *Infrared and Raman Selection Rules for Molecular and Lattice Vibrations: The Correlation Method*; J. Wiley and Sons: New York, 1972.
- (11) Poojary, D. M.; Shpeizer, B.; Clearfield, A. *J. Chem. Soc., Dalton Trans.* **1995**, 111–113.

Table 2. Infrared and Raman Frequency (cm^{-1}) and Assignment of the Vibrational Modes of the $\gamma\text{-M}[\text{PO}_4][\text{O}_2\text{P}(\text{OH})_2]\cdot\text{H}_2\text{O}$ Species (M = Ti, Zr)

Ti		Zr		assignment	
infrared	Raman	infrared	Raman	vibrational character	unit
3556 m		ca. 3480 m, br		$\nu(\text{PO}-\text{H})$	$[\text{O}_2\text{P}(\text{OH})_2]$
3460 m					
1585 m		ca. 1625 m, br		$\delta(\text{H}-\text{O}-\text{H})$	H_2O
1231 m		ca. 1244 m, sh		$\delta(\text{P}-\text{O}-\text{H})$	$[\text{O}_2\text{P}(\text{OH})_2]$
ca. 1184 w, br		1223 m			
	ca. 1119 w, br	ca. 1142 m, sh	1145 m	$\nu(\text{P}-\text{O})_{\text{as}}$	$[\text{O}_2\text{P}(\text{OH})_2]$
	1080 m	1085 s	1093 m		$[\text{O}_2\text{P}(\text{OH})_2] + [\text{PO}_4]$
1059 vs	ca. 1040 m, br		1076 w		
999 s	1005 vs	ca. 1022 s, sh	1029 vs	$\nu(\text{P}-\text{O})_{\text{s}}$	$[\text{O}_2\text{P}(\text{OH})_2]$
	984 vs		1006 s		$[\text{PO}_4]$
ca. 956 vs, br		991 vs, br		$\nu(\text{P}-\text{OH})_{\text{as}}$	$[\text{O}_2\text{P}(\text{OH})_2]$
	936 m	ca. 938 m, br	942 m	$\nu(\text{P}-\text{OH})_{\text{s}}$	$[\text{O}_2\text{P}(\text{OH})_2]$
ca. 725 m, br				$\gamma(\text{H}-\text{O}-\text{H})$	H_2O
630 w	636 w, br	637 m	636 mw	$\delta(\text{O}-\text{P}-\text{O})$	$[\text{PO}_4]$
618 w					
	ca. 490 vw, br	522 m	516 mw		$[\text{PO}_4] + [\text{O}_2\text{P}(\text{OH})_2]$
	421 m		421 m	$\nu(\text{M}-\text{O})_{\text{s}}$	$[\text{MO}_6]$
	376 m, br		366 w	$\delta(\text{O}-\text{P}-\text{O}) + \delta(\text{O}-\text{P}-\text{OH})$	$[\text{PO}_4] + [\text{O}_2\text{P}(\text{OH})_2]$
			349 w		
			311 m		
	270 m		ca. 256 m, br	$\nu(\text{M}-\text{O})_{\text{as}} + \text{lattice vibr}$	$[\text{MO}_6]$
			188 w		

**Figure 1.** Reflection microscopy infrared (dashed line) and Raman (solid line) spectra of $\gamma\text{-ZrP}$ species.

internal vibrational modes of the PO_4 group (Table 2) transform into nine A modes in site C_1 ; moreover, by taking into account the multiplicity of the PO_4 unit in the Bravais cell and the factor group symmetry, a pattern of 18 vibrational modes ($9A + 9B$, all infrared- and Raman-active) is expected. Referring to the H_2PO_4 unit, the 15 modes transform in the site symmetry into 15 A modes and by the factor group symmetry into an expected pattern of 30 vibrational bands ($15A + 15B$). Summing up together all the contribution of the intramolecular vibrations of the phosphate units, 48 bands are expected, all infrared- and Raman-active, which, apart from the four $\nu(\text{OH})$ modes, are collected in a short spectral range between 1300 and 400 cm^{-1} . Figure 1 illustrates this section of the spectra. The infrared pattern in particular is characterized by a broad, structured absorption centered at ca. 1000 cm^{-1} , which, on one side, underlines the extended dipolar–dipolar coupling between the IR-active molecular modes and, on the other side, discourages any attempt at assignment on the basis of

crystal vibrational analysis. Similar consideration can be drawn from the analysis of the $\alpha\text{-Zr}$ material, whose structural data¹² [formula, $\text{Zr}(\text{HPO}_4)_2(\text{H}_2\text{O})$; crystal system, monoclinic; space group, $P2_1/b$ (C_{2h}^5); site symmetry, $C_1(2)$, $C_1(4)$; and $Z = 4$] give rise to 48 internal vibrational modes of the HPO_4 units, distributed into $12A_g + 12A_u + 12B_g + 12B_u$.

The Raman spectra, on the contrary, show a much simpler vibrational pattern, with a very neat intensity distribution profile, which suggests a substantial absence of coupling effects in the crystal. This is not surprising, as our experience on solid-state spectra of metal carbonyl clusters¹³ indicates, that while coupling can occur between induced dipoles within the molecular units in the crystal, much less frequent are coupling phenomena between quadrupole moments occurring when Raman-active vibrations are concerned.

The above considerations suggest that the Raman features can be tentatively approached by use of the zeroth-order approximation. That is, the vibrations of the isolated ions or molecules in the lattice may be treated according to their molecular point group, considering a small or negligible effect of both the site symmetry and the factor group symmetry. The infrared spectra are useful to confirm and complete the assignment.

The vibrational study on phosphate species ($[\text{PO}_4]$, $[\text{O}_3\text{POH}]^{2-}$, and $[\text{O}_2\text{P}(\text{OH})_2]^-$ units) appeared in the literature more than 30 years ago.¹⁴ At that time, laser Raman spectroscopy was in its infancy; therefore, we have found it useful to check again the vibrational pattern of some

(12) Troup, J. M.; Clearfield, A. *Inorg. Chem.* **1977**, *16*, 3311–3313.(13) (a) Kettle, S. F. A.; Diana, E.; Rossetti, R.; Stanghellini, P. L. *J. Am. Chem. Soc.* **1997**, *119* (35), 8228–8231. (b) Kettle, S. F. A.; Diana, E.; Rossetti, R.; Stanghellini, P. L. *Inorg. Chem.* **1998**, *37* (25), 6502–6510. (c) Kettle, S. F. A.; Diana, E.; Boccaleri, E.; Stanghellini, P. L. *Eur. J. Inorg. Chem.* **1999** (11), 1957–1963.(14) (a) Von Steger, E.; Herzog, K. *Z. Anorg. Allg. Chem.* **1963**, *331*, 169. (b) Von Steger, E.; Herzog, K.; Klosowski, J. *Z. Anorg. Allg. Chem.* **1977**, *432*, 42.

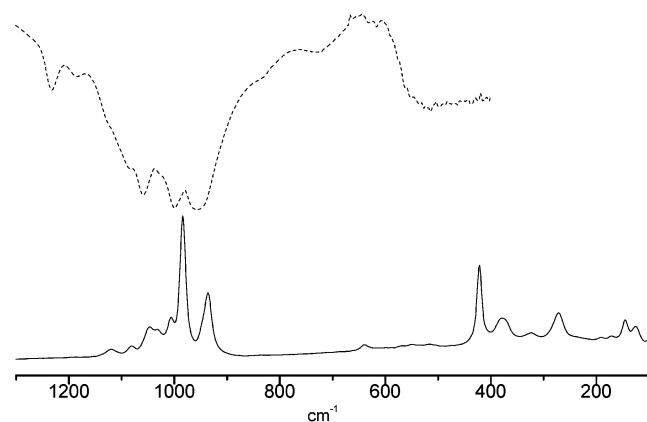


Figure 2. Reflection microscopy infrared (dashed line) and Raman (solid line) spectra of γ -TiP species.

potassium phosphate salts, such as K_3PO_4 , K_2HPO_4 , and KH_2PO_4 in crystals and, in particular, in water solution. The solutions were all obtained by starting from 40% (w/v) H_3PO_4 and adding appropriate amounts of KOH. Each phosphate species reaches the maximum concentration when pH is intermediate between the pK_a values of phosphoric acid system, that is, 4.45 for $[O_2P(OH)_2]^-$, 9.75 for $[O_3POH]^{2-}$, and greater than 13 for $[PO_4]$.

These vibrational data and their assignment, which do not substantially differ from those reported in the literature, form the basis of the interpretation of the more complex spectra of the layered materials. It should be underlined that

(i) the frequency of the antisymmetric $\nu(P-O)$ modes lies in a range ($1100-1000\text{ cm}^{-1}$) greater than that of the corresponding symmetric $\nu(P-O)$ modes ($950-900\text{ cm}^{-1}$),

(ii) the frequency of the $\nu(P-OH)$ modes is lower than that of the $\nu(P-O)$ modes of the same symmetry (ca. 850 cm^{-1} vs ca. 950 cm^{-1}), and

(iii) the range of the $\delta(P-O-H)$ modes is well established at ca. $1300-1200\text{ cm}^{-1}$.

Moreover, the infrared and Raman intensities are useful guides for the assignment. As an example, all the antisymmetric $\nu(P-O)$ modes are expected to have great infrared and weak Raman intensities, as formally derived from the tetrahedral T_2 mode. The opposite will occur with the symmetric $\nu(P-O)$ modes, formally derived from the A_1 mode.

The complete set of the vibrational data of the γ -Ti(Zr)P layered systems are reported in Table 2, while Figures 1 and 2 illustrate their vibrational patterns; the related assignment seems to be straightforward. Data and spectra concerning the α -Ti(Zr)P systems have been more or less detailed in the literature¹⁵ and are collected in the Supporting Information (Table S1, Figures S1 and S2).

Alongside, some interesting comments can be done:

(i) The very strong and very broad infrared band, centered at ca. 1000 cm^{-1} and common to all the spectra, is due to

the antisymmetric (P–O) stretching, which clearly feels the site/factor group effects of the crystal. These effects are reduced or absent in the Raman spectra, which allows a more confident assignment.

(ii) The contemporaneous presence of two units, $[PO_4]$ and $[O_2P(OH)_2]$, causes probable overlaps among the $\nu(P-O)$ modes and among the $\delta(O-P-O)$ modes belonging to them. The stretching modes of $[O_2P(OH)_2]$ have higher frequency than those of $[PO_4]$, whereas the bending modes of the two units have opposite trends.

(iii) The $\nu(O-H)$ and the $\nu(P-OH)$ modes of the two α -compounds appear as doublets, in agreement with the presence of two crystallographically nonequivalent O_3POH groups in the asymmetric unit,³ although the effect of different hydrogen bonds with the interlayer water molecules cannot be excluded.

(iv) Among the M–O stretching modes, the formally A_{1g} (totally symmetric) mode is expected as sharp medium-strong band in the Raman spectrum, as often it occurs for the octahedral MX_6 systems.¹⁶ Looking to the spectra, the only possible candidate is the band around 300 cm^{-1} for the α -species and around 400 cm^{-1} for the γ -species. Even though also some bending modes of the phosphate units can lie in the same region, we are confident on the correctness of the assignment, also taking into account that similar features do not appear at all in any spectrum of the potassium phosphate salts.

Discussion

Layered phosphate systems show a vibrational pattern that can be related to the phosphate units constituting their structure. However, despite the molecular treatment that could seem a rough but reasonable approximation, this can give account, when compared with the spectra of alkali phosphates, of some observed peculiarities.

The most intriguing problem is the general shift toward high energy of the $\nu(P-O)$ modes of the layered species, with respect to those of the simple alkali phosphate in solution or in the solid state. The shift is significant, around $70-80\text{ cm}^{-1}$ as similar groups are compared, although the bond lengths of the layered systems lie in the same range ($1.50-1.56\text{ \AA}$) as the alkali phosphates.^{3,4,17} As an example, for $[PO_4]$ unit the Raman frequency of the totally symmetric mode is $1006/970\text{ cm}^{-1}$ (γ -Zr/Ti) and 924 cm^{-1} (K_3PO_4), and for the $[O_3POH]$ unit is $1052/996\text{ cm}^{-1}$ (α -Zr/Ti) and 949 cm^{-1} (K_2HPO_4). Such different frequencies do not correspond to parallel different P–O bond distances. Very likely, the frequency variation reflects a subtle modification of the P–O bond, induced by the extent of the M(Zr,Ti)–O interaction.

When general systems $M'_x[EO_n]$ ($E = N, P, S$, etc.) are considered, the effect of the cation M' in the E–O stretching

(15) Slade, R. C. T.; Knowles, J. A.; Jones, D. J.; Rozière, J. *Solid State Ionic* **1997**, *96*, 9. (b) Slade, R. C. T.; Forano, C. R. M.; Pressman, H. A.; Nicol, J. M.; Peraio, A.; Alberti, G. *J. Mater. Chem.* **1992**, *2*, 583. (c) Colombari, P.; Novak, A. *J. Mol. Struct.* **1989**, *198*, 277. (d) Horsley, S. E.; Nowell, D. V.; Stewart, D. T. *Spectrochim. Acta* **1974**, *30A*, 535

(16) (a) Corsit, A. F.; Hoefdraad, H. E.; Blasse, G. *J. Inorg. Nucl. Chem.* **1972**, *34*, 3401. (b) Hauck, J.; Fadini, A. *Z. Naturforsch.* **1970**, *25b*, 422. (c) Hauck, J. *Z. Naturforsch.* **1970**, *25b*, 468.

(17) (a) Morosin, B.; Samara, G. A. *Ferroelectrics* **1971**, *3*, 49. (b) Lis, T. *Acta Crystallogr. C* **1994**, *50*, 484. (c) Choudhary, R. N. P.; Nelmes, R. J.; Rouse, K. D. *Chem. Phys. Lett.* **1981**, *78*, 102. (d) Wiench, D. M.; Jansen, M. *Z. Anorg. Allg. Chem.* **1980**, *461*, 101.

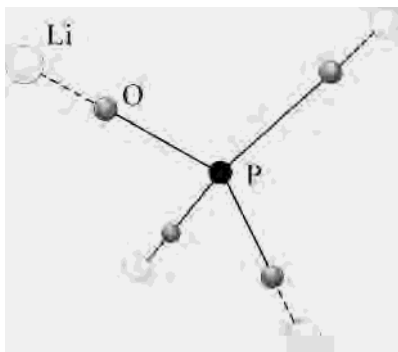


Figure 3. Structural model of the $\text{Li}_4[\text{PO}_4]$ theoretical system.

frequency has been a debated and still unresolved problem. First of all, depending on the polarizability of M' (given usually by q^2/r , where q is the charge and r is the radius), the $M'-\text{O}$ interaction can be taken as purely electrostatic or as a true covalent bond, the last case with M' having a very low q^2/r value. Irrespective of the nature of this interaction, a common behavior is expected; that is, an increase of the $M'-\text{O}$ interaction corresponds to a decrease of $E-\text{O}$ bond and, consequently, a decrease of the $\nu(E-\text{O})$ frequency.¹⁸ The expectation is sometimes fulfilled, but in other cases no correlation has been found between the frequency and any parameter concerning M' ,¹⁹ or even the opposite relationship has been reported, that is, the more polarizing cation gives rise to the higher frequency.

We have tentatively approached to this problem by making use of a theoretical model $[\text{Li}_4\text{PO}_4]^+$ (Figure 3) that consists of a tetrahedral $[\text{PO}_4]$ unit with four Li^+ approaching along the $\text{P}-\text{O}$ direction. In the calculation the geometry of the $[\text{PO}_4]$ unit is maintained fixed, whereas the $\text{Li}-\text{O}$ distance is systematically changed until it reaches the distance corresponding to the average bond distance in the salt Li_3PO_4 .²⁰ We are aware that Li can poorly simulate the $\text{Zr}(\text{Ti})-\text{O}$ interaction in the solid-state frame. Our purpose, however, is not to offer a good theoretical model for the vibration in the crystal but simply to have a qualitative explanation of the trend of $\nu(\text{P}-\text{O})$ vs $M'-\text{O}$ distance. In that respect Li^+ is appropriate as it can simulate a partial covalent character, which is expected from the $\text{Zr}(\text{Ti})-\text{O}$ interaction.

The main results of the calculation are collected in Table S2 (Supporting Information). A trend in the Mulliken atomic charge partition, with the necessary care due to the limitations of this method of population analysis, is clear: when Li is moved closer to O , an increased electron charge moves from O to Li , suggesting an increased covalence of the $\text{Li}-\text{O}$ interaction. This is accompanied by a lowering of the energies of the highest occupied molecular orbital (HOMO) and of the nearest filled molecular orbitals, as shown by the Walsh-like diagram, illustrated in Figure 4. Some of these molecular orbitals are essentially localized on the oxygen

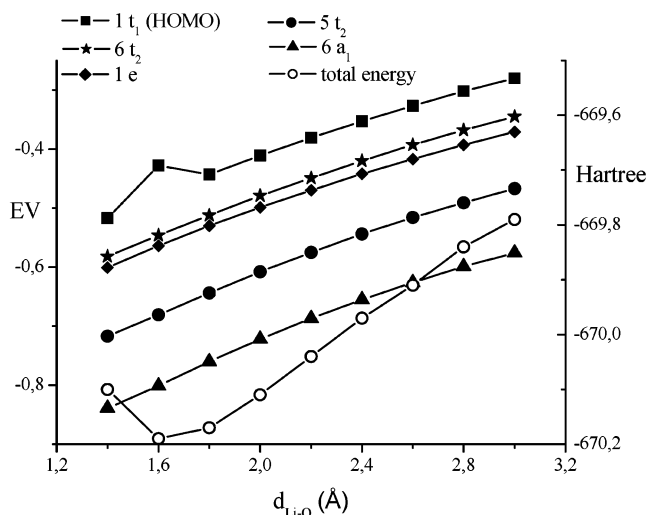


Figure 4. Walsh-like diagram of the energy of the molecular orbital (scale on the left) and of the total energy (scale on the right) vs the $\text{Li}-\text{O}$ bond distance.

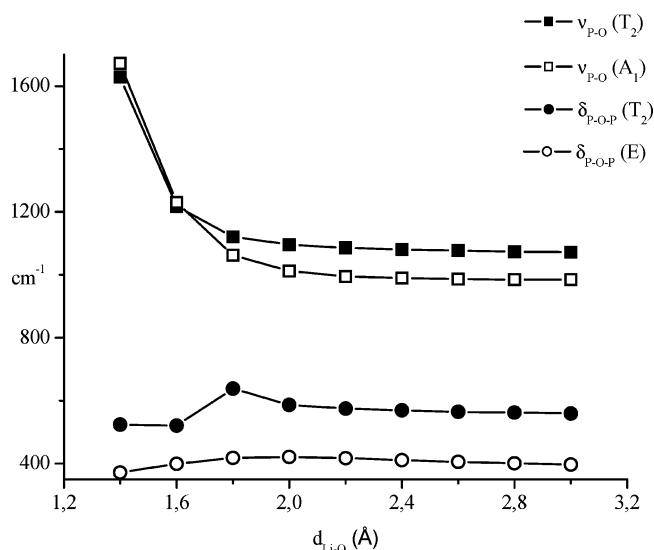


Figure 5. Walsh-like diagram of the $\nu(\text{P}-\text{O})$ and $\delta(\text{O}-\text{P}-\text{O})$ frequency values vs the $\text{Li}-\text{O}$ bond distance.

atoms ($1 t_1$, $6 t_2$, and $1 e$), but some others ($5 t_2$ and $6 a_1$) have a significant $\text{P}-\text{O}$ bonding contribution. The trend is evident: when the $\text{Li}-\text{O}$ distance decreases, the $\text{Li}-\text{O}$ interaction increases, which causes a stabilization of the frontier molecular orbitals, in particular those having $\text{P}-\text{O}$ bonding character. So, all the bonds of the $\text{Li}-\text{O}-\text{P}$ unit are reinforced, and as a consequence, the $\text{P}-\text{O}$ stretching frequencies are increased (see Figure 5). These plots also show that the frequency order $T_2 > A_1$ is maintained, according to the experimental data, at least in a reasonable range of $\text{Li}-\text{O}$ distances.

The covalence of the $\text{Zr}(\text{Ti})-\text{O}$ interaction is supported by the clear appearance of the totally symmetric $\nu(\text{M}-\text{O})$ stretching mode in the Raman spectra. The frequency values of 291 cm^{-1} (Zr) and 310 cm^{-1} (Ti) for the α -species and 421 cm^{-1} (Zr) and 407 cm^{-1} (Ti) for the γ -species are much lower than the values reported for MO_6 metal oxides ($700-800 \text{ cm}^{-1}$).¹¹ This may be ascribed in part to the mass effect of the ligand ($[\text{PO}_4]$ unit instead of O) but especially to the

(18) Muller, A.; Baram, E. J.; Carter, R. O. *Struct. Bond.* **1976**, *20*, 81

(19) (a) Hezel, A.; Ross, S. D. *Spectrochim. Acta* **1966**, *22*, 1949. (b)

Ferraro, J. R.; Walker, A. *J. Chem. Phys.* **1965**, *42*, 1273 and 1278.

(c) Walrafen, G. E. *J. Chem. Phys.* **1965**, *43*, 479.

(20) Wang, B.; Chakoumakos, B. C.; Sales, B. C.; Kwak, B. S.; Bates, J. B. *J. Solid State Chem.* **1995**, *115*, 313.

higher M–O bond order in the isolated MO_6 species (extended π -effect) with respect to the same group in layered compounds, where the interaction is obviously much weaker.

It is interesting to note that $\nu(\gamma\text{-species})$ are greater than $\nu(\alpha\text{-species})$, which is in line with the slightly shorter Zr–O distances (2.040 vs 2.064 Å). Finally, the frequencies are quite insensitive to the metal atom, as expected for a mode, A_{1g} , that in an ideal symmetry does not imply the motion of the central atom.

Conclusion

The vibrational spectra of layered metal phosphates have been approached by the correlation method in the solid state to analyze the spectroscopic behavior. The expected profile, due to the extremely low site symmetry for the phosphate units, is much more complex than in particular the experimental Raman spectra. A zeroth-order approximation, considering the system on a molecular basis, can provide a reasonable interpretation of the vibrational features of these layered materials in comparison to model alkali phosphate salts. This approach can allow interesting correlations

between vibrational and structural data. These considerations have been also verified by a quantomechanical model that has led to an affordable description of the effect of the interaction between the phosphate units and the cationic M^{4+} species in the structures.

Since many other metal phosphate and phosphonate materials of interest may be built by tetrahedra–octahedra block connections, Raman spectroscopy can be usefully used to obtain important insights on the composition, structure, and properties of these materials, especially when single crystals of suitable size for X-ray structural determination are not available.

Supporting Information Available: Infrared and Raman frequency and assignment of the vibrational modes of the $\alpha\text{-M}[\text{O}_3\text{POH}]_2\cdot\text{H}_2\text{O}$ species ($M = \text{Ti}, \text{Zr}$) (Table S1) and the results of the theoretical calculation on $\text{Li}_4[\text{PO}_4]$ model (Table S2), and reflection microscopy infrared and Raman spectra of $\alpha\text{-ZrP}$ species (Figure S1) and of $\alpha\text{-TiP}$ species (Figure S2). This material is available free of charge via the Internet at <http://www.pubs.acs.org>.

IC049565C